

# WIND EFFECTS ON FLAME SPREAD AND EMBER SPOTTING NEAR A STRUCTURE

Kathryn M. Butler, Erik Johnsson, Marco Fernandez, Mariusz Zarzecki, Eric Auth, and Glenn Forney  
Fire Research Division, Engineering Laboratory  
National Institute of Standards and Technology  
Gaithersburg, MD 20899-8662 USA

## ABSTRACT

In wildland-urban interface (WUI) fires, combustible materials pose a potential threat to contiguous or nearby structures. Flame spread and firebrand spotting have been studied in a series of field experiments involving mulch beds under a variety of wind conditions and separation distances from a small structure. The rate of flame spread in a mulch bed was observed to slow significantly as the fire approached the structure, with flame contact with the structure occurring only after the gap was jumped by firebrand spotting. Computational fluid dynamics (CFD) modeling was used to gain insight into the flow field. A vortex forming near the base of the structure in the wind field was found to be responsible for changing the flame spread from a concurrent flow situation to opposed flow as it approaches the structure.

## INTRODUCTION

In wildland-urban interface (WUI) fires, combustible materials pose a potential threat to contiguous or nearby structures. The wind field around a structure affects the behavior of a fire in its vicinity, including the flame spread over fuels near the structure and the trajectory and accumulation of firebrands. Fire propagation over mulch and other ground fuels is strongly affected by the flow field near the ground. In concurrent flame spread, with the wind flow in the same direction as the flame spread, the rate of flame spread is strongly affected by radiative and convective heat transfer between the flame and the unburned fuel bed.<sup>1</sup> As the wind (or slope) increases, the angle between the flame and the unburned fuel decreases, and the dominant mechanism of preheating changes from radiation to convection as buoyancy forces become weaker than inertial forces.<sup>2,3</sup> For opposed flow, or creeping, flame spread, gas phase chemical kinetics play a leading role, and the heat transfer between the flame and unburned fuel is limited to a small region in which the material is heated to pyrolysis temperatures.<sup>1,4</sup> Opposed flow flame spread is therefore much slower than concurrent flame spread. For concurrent flow, the flame spread rate over packed natural fuel beds has been found to be roughly linear with wind speed.<sup>5</sup>

The flow fields around surface-mounted rectilinear objects have been studied by a number of researchers. The shed structure used in this set of experiments closely resembles a cube, which has been well studied. Hunt et al.<sup>6</sup> developed a sketch of the flow pattern around a cube oriented perpendicular to the flow, based on wind tunnel experiments and topological considerations. At high Reynolds number ( $Re \approx 10^4$ ), a vortex wrapped around the structure near the ground in a horseshoe pattern is observed upstream of the object. Note that a ground fire approaching a structure under these conditions would go from a region of concurrent flow to a region of opposed flow as the flames encounter the vortex. Depending on the flow parameters, additional smaller counter-rotating vortices may add to the complexity of the upstream flow. These vortex patterns were confirmed by Martinuzzi and Tropea<sup>7</sup> in flow visualization experiments at  $Re \approx 10^5$ . The upstream separation distance was found to be about 0.8 times the height of the object  $H$  for a cube. A numerical study of a wall-mounted cube in channel flow by Sedighi and Farhadi<sup>8</sup> showed that the number of upstream vortices decreases as  $Re$  increases from 1000 to 40 000. The upstream separation distance

reached a maximum of about  $1.8 H$  at  $Re = 10\,000$  and a minimum of  $0.9 H$  at  $Re = 40\,000$ .

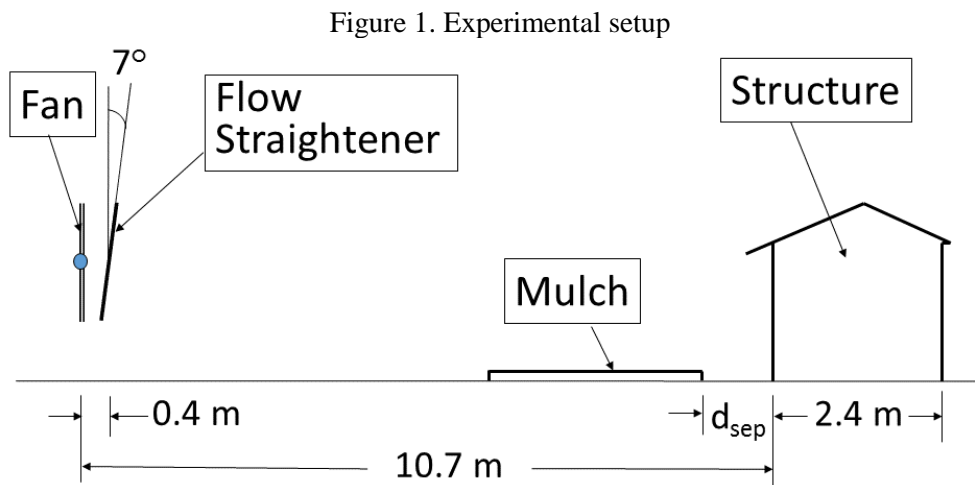
This paper reports on a series of field experiments on flame spread and firebrand spotting over shredded hardwood mulch under a variety of wind conditions and separation distances from a nearby structure. A simulation of the flow fields in this set of experiments is used to provide insight into the characteristics of the flame spread rates. The experiments described in this paper are part of a larger study that includes multiple mulch types and a variety of fence types placed within the mulch bed.

## EXPERIMENTS

A series of experiments was performed to observe the behavior of fire over a bed of shredded hardwood mulch. Both the movement of the flame front and spotting from firebrands generated by the mulch were of interest. Researchers from the National Institute of Standards and Technology (NIST) carried out these experiments at the Frederick County Fire and Rescue Training Facility in Maryland, U.S.A.

### Experimental setup

Figure 1 shows the configuration for this set of experiments. The mulch bed consisted of a  $0.05\text{ m}$  thick layer of shredded hardwood mulch packed within a steel pan  $0.91\text{ m}$  wide and  $3.4\text{ m}$  long, with  $0.04\text{ m}$  high sides. Since a single pan of the required length was not available, the mulch pan consisted of two overlapping pans nested together, with the end pieces folded down to make a single unit. The mulch bed was arranged perpendicular to the side wall of a small structure  $2.44\text{ m}$  on a side. A sacrificial piece of T1-11 plywood siding covered the bottom  $1.2\text{ m}$  of the wall facing the mulch bed. The separation distance  $d_{\text{sep}}$  between the mulch bed and the structure was varied from  $0\text{ m}$  to  $6\text{ m}$ . In some cases, a separate pan  $0.46\text{ m}$  wide and containing a  $0.05\text{ m}$  thick layer of shredded hardwood mulch was placed along the base of the structure, perpendicular to the mulch pan, in order to observe ignitions from firebrands generated by the burning mulch. In these cases, the plywood layer over the wall of the structure was replaced with a non-combustible surface (cement board) for better protection.



The wind field was generated by a large fan (a gas-engine powered propeller)  $2.1\text{ m}$  in diameter located  $10.7\text{ m}$  from the structure. A flow straightener tilted at  $7^\circ$  directed the flow toward the mulch bed. Figure 2 shows the experimental setup from a viewpoint to the right and behind the fan. Wind speed was measured and recorded using a set of 13 bidirectional pressure probes in an array mounted  $1.22\text{ m}$  in front of the mulch bed. Five probes were arranged vertically along the centerline of the experiment, and 5 probes (including the one along the centerline) were located in a horizontal line  $1.22\text{ m}$  above the ground. The other 4 probes were located along top and bottom rods of the probe array.

Figure 2. Experimental setup showing fan and flow straightener aiming wind flow toward mulch pan and structure

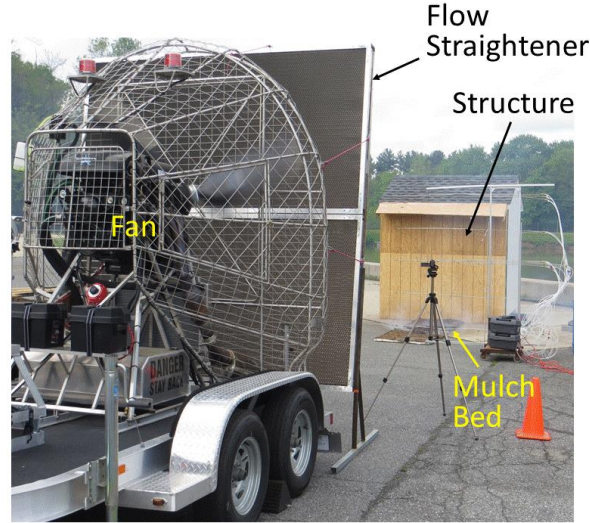
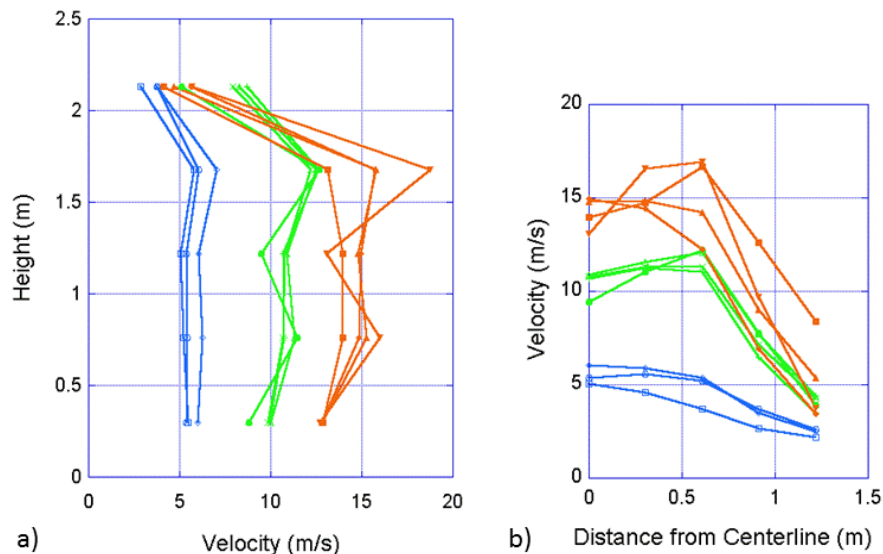


Figure 3 shows average wind velocity profiles from bidirectional probes arranged along vertical and horizontal lines. The plots show values at each probe time-averaged over the entire experiment, from sample experiments conducted on different test days. The fan was nominally set to deliver steady wind speeds of 6 m/s (blue), 10 m/s (green), and 14 m/s (red). The plots in Fig. 3a show that the value of average velocity at the lowest location was the most repeatable, that the repeatability of the average velocity worsened with height, and that the value of average velocity at the highest location dropped significantly. Except for one case with a wind speed setting of 14 m/s, the vertical profile was reasonably uniform from 0.3 m through 1.7 m in height. Assuming that the horizontal profile in Fig. 3b was symmetric, the flow speed was reasonably uniform over the 0.91 m width of the mulch bed.

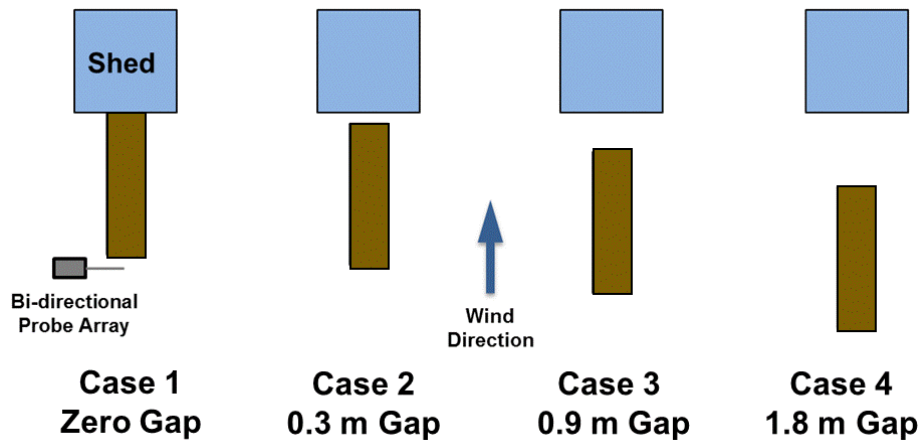
In order to maintain the specified wind over the entire length of the mulch bed and to the wall of the structure, experiments were carried out only when the speed of the ambient wind was lower than 1/3 times the required wind flow from the fan.

Figure 3. Average wind velocity profiles from bidirectional probe array a) along vertical line at centerline of mulch bed and b) at 1.22 m height above ground



The configurations in Fig. 4 show the four separation distances that were tested:  $d_{\text{sep}} = (0, 0.3, 0.9, 1.8) \text{ m}$ . Without a separate mulch bed sitting at the base of the structure, the zero separation distance case was the only configuration that allowed direct contact between the burning mulch and the wall of the structure. The flames over the mulch bed were not high or intense enough to cause ignition by radiation. Therefore, without contact between the burning mulch and the structure, firebrands were the only way to ignite the plywood layer. This required the firebrands to either be caught in a crevice underneath the structure or accumulate at its base.

Figure 4. Top view of mulch bed layouts



The behavior of the mulch bed after ignition was captured in four cameras; two were located with a view of the mulch bed from the right or left side, and two were positioned on either side of the wind machine with a near end-on view of the mulch bed. At least one camera had a clear view of the digital clock on the right side of the structure that was the official timekeeper of the experiment.

### Experimental procedure

Before each experiment, the mulch was dried on pallets in the sun or in aerated barrels until samples taken from multiple sites measured less than 7 % moisture content using a moisture analyzer. The mulch bed was prepared by positioning the steel pan in front of the structure and filling the pan with an even layer of shredded hardwood mulch, which was lightly compressed by foot. Then the mulch was ignited with a propane burner placed on the mulch bed near the end closest to the fan. The burner was left in place for 1½ min to allow the fire to become established. After the burner was removed, the engine driving the fan was started and brought up to speed. The progress of the fire was observed until ignition or charring was observed somewhere along the outer sacrificial layer of the structure, at which point the mulch and all firebrands were extinguished with water.

### EXPERIMENTAL ANALYSIS

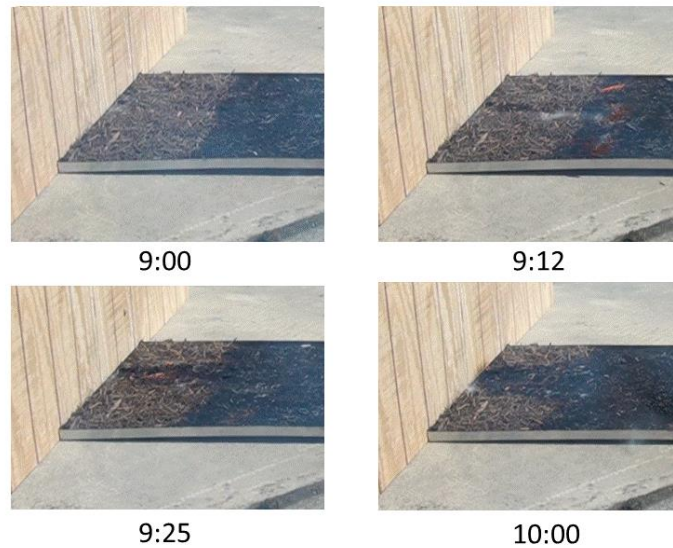
The modes of fire progression over the mulch bed can be separated into flame spread, which moves the fire continuously from the point of ignition into unburned material, and firebrand spotting, which ignites new fires at some distance away from the fire front.

In every mulch experiment, the flame spread was observed to slow significantly as the flame front approached the structure wall, with the first ignition of the plywood layer resulting in each case from a firebrand landing in and igniting the mulch at a point much closer to the wall than the fire front. Figure 5 shows a particularly clear example of this phenomenon. The photo at 9:00 shows the position of the flame front that has stalled near the wall of the structure. At this time a firebrand has just landed very close to the

wall and ignited the mulch. From this second point of ignition, flames spread toward the wall and eventually ignite the plywood. In the other direction, within 12 s the flames from this second ignition point have burned in a line back toward the original flame front, as shown in the top right photograph. The flame front then spreads laterally from the burned line, while the original flame front continues to move forward very slowly.

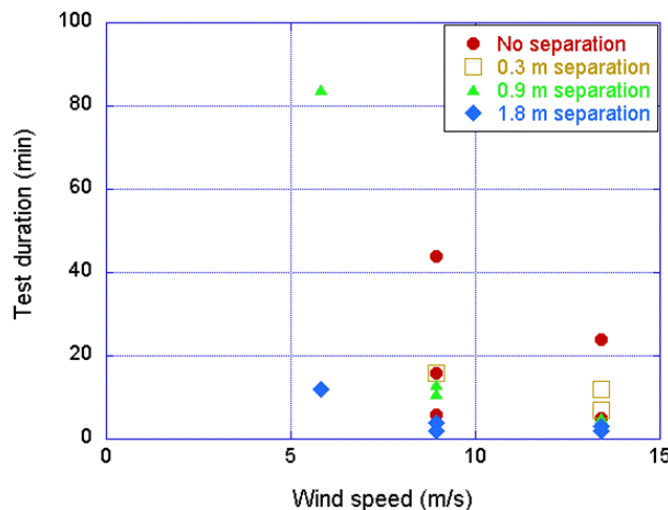
Other phenomena were observed to affect the rate of flame spread in the mulch experiments. In many experiments, a firebrand ignited the mulch downstream of the main flame front, creating a separate burning region that expanded with time until the flame front merged with the upstream edge of the main flame front. This resulted in jumps in the flame front location.

Figure 5. Mulch experiment in 10 m/s imposed flow, showing the evolution of the flame front due to spotting from a firebrand igniting mulch next to the wall



An assessment of the number of minutes between the time of removal of the propane burner and the time when the flame front reached the end of the mulch bed resulted in the plot of test duration as a function of fan wind speed and separation distance shown in Fig. 6. This indicates that experiments take less time (the flame spread is faster) as the wind speed increases and as the separation distance increases from 0 m to 1.8 m. Some anomalous results are seen for the zero separation distance cases.

Figure 6. Test durations for all shredded hardwood mulch experiments



Further investigation of the behavior of the flame front required more detailed analysis of the video recordings of the experiments and a qualitative look at the flow field using computational fluid dynamics (CFD).

### Video analysis

The position of the flame front as a function of time for a given experiment was determined from a set of frames extracted from the video recorded by the right or left camera or both. Each camera view was fixed in place during the experiment after having been adjusted beforehand to capture the field of interest. To measure the position of the flame front in a given frame, a physical scale was developed using a set of perspective lines created for each camera view. Figure 7 gives an example, with lines marked off in units of feet. The set of perspective lines in this frame make it possible to estimate distances from the structure wall, including the position of the flame front closest to the wall. The lines were generated using MATLAB\* software by selecting two points on top of the mulch at each end of the mulch pan and setting a physical scale from a known distance. In this case, the corner of the white square marking on the asphalt in the foreground was known to be  $3\frac{1}{2}$  ft (1.07 m) from the wall. In later experiments, markings added to the pavement made it easier to determine both the physical scale and the angle of perspective lines along the length of the mulch bed.

For camera views in which the upstream end of the mulch pan was not in the frame, as was the case for some of the experiments with 0.9 m and 1.8 m separation distances, the perspective line away from the structure was established using other information. On a sunny day, such as that shown in Fig. 7, the shadow cast by the bidirectional probe array could be used, assuming that the array had been positioned parallel to the wall. In cases in which the mulch pan was separated from the wall, the location of the perspective line along the wall at mulch height was estimated.

Figure 7. Perspective lines to track the flame front superimposed on a video frame



\* Certain commercial products are identified in this paper in order to specify the experimental procedure adequately. Such identification is not intended to imply recommendation or endorsement by the National Institute of Standards and Technology, nor is it intended to imply that the products identified are necessarily the best available for the purpose.

The boundary between burned and unburned mulch was considered to be where the color of the mulch changed from brown to black. Flames attached to the mulch were observed in some video frames but were too sporadic to serve as an indicator of flame front location. The flame front was typically not a straight line. The leading edge of the flame front was therefore defined as the point of the continuous burn pattern closest to the structure. On occasion, burn spots appeared in the mulch bed downstream of the flame front due to firebrands. When a spot became connected to the main burned region, the location of the flame front jumped to the leading edge of the spot, which was then incorporated into the main burning region. For the plots in this paper, the initial time  $t = 0$  s was taken as the time when the propane burner was removed.

The measurement of the flame front location was subject to uncertainty from both setting the physical scale and determining the leading edge of the flame front. Sources of uncertainty were all Type B, with standard uncertainty based on scientific judgment. The perspective line at mulch height along the wall could be incorrect by  $\pm 0.5$  cm for zero separation cases, due to uneven piling of mulch against the wall and distortions in the mulch pan, and as much as  $\pm 2$  cm for experiments with nonzero separation distances, for which the position was estimated. The accuracy of the points defining the perspective line far from the structure was estimated as  $\pm 1$  cm when the end of the mulch pan was visible in the frame and  $\pm 4$  cm when it was not. Other minor sources of uncertainty included lens distortions in the camera, which may throw off the assumption of linearity used to create the set of perspective lines, and wind vibrations that caused the image to move under the superimposed lines.

Determining the location of the flame front was challenging in many cases. The contrast between burned and unburned areas depended on the lighting on sunny or cloudy days and on the presence of smoke and flames in the image. Frames in which the smoke or flames completely obscured the flame front were skipped. The inhomogeneity of the shredded hardwood mulch also added to the difficulty of determining the location of the flame front. This source of uncertainty was estimated to be on the order of  $\pm 3$  cm.

The combined standard uncertainty in the flame front location, calculated as the square root of the sum of squares from all of these sources, was  $\pm 5.5$  cm. An analysis of the videos from both right and left cameras from a single experiment provides a test of this estimate of uncertainty. Examples will be pointed out in the plots in the next section.

### **Flame front locations**

Figure 8 shows the flame front location as a function of time for an experiment in which the mulch bed was separated from the structure by a distance of 0.9 m and subjected to an imposed wind set to 6 m/s. The flame spread rate is given by the slope of this plot. This plot demonstrates the main features observed in many of these mulch experiments. Initially there is a start-up period, during which the burning region expands from the area under the propane burner toward the edges of the pan. The spread rate of the flame front toward the wall of the structure is slower during this time period, which in this case is from 0 s to about 500 s. The flame spread rate then increases, and is constant or gradually decreasing until it reaches a location, here about 1.6 m from the wall, where there is an abrupt decrease. The flame spread rate is then constant at this lower value except for locations where firebrand spotting causes a jump in the location. In this case, a change in the flame spread rate due to spotting does not occur until the flame front is nearly at the end of the mulch bed at 0.9 m from the wall.

Figure 8. Flame front location with time for separation distance of 0.9 m and wind speed of 6 m/s

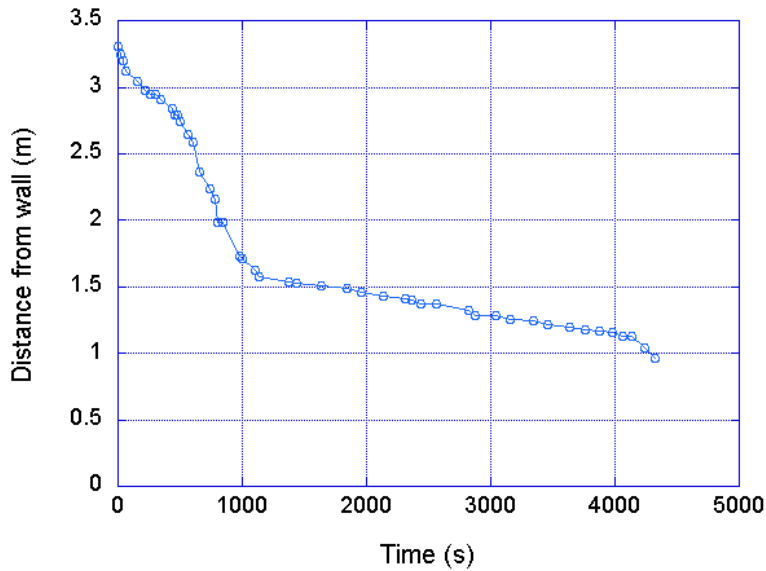
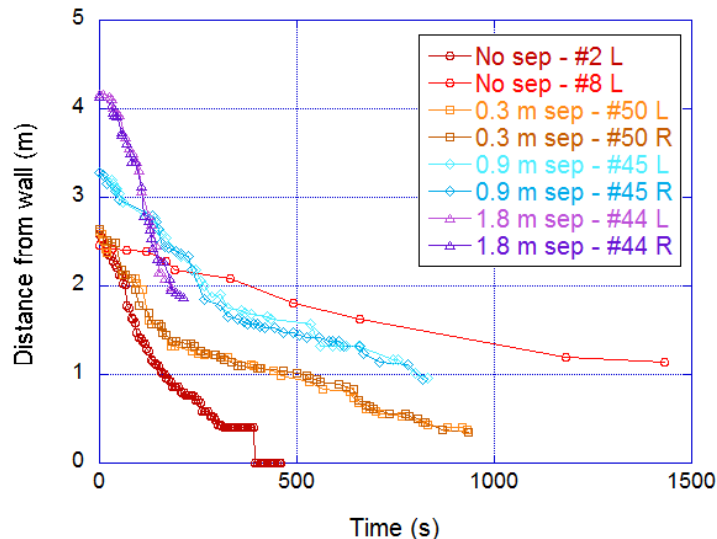


Figure 9 shows flame front locations relative to the structure wall for a set of experiments at various separation distances, with the fan set to deliver a wind speed of 10 m/s. Note that the behavior for 0.3 m and 0.9 m separation distances is similar. In both cases, the flame spread rate is relatively constant until the flame front reaches about 1.4 m from the wall in the 0.3 m separation case and about 1.7 m from the wall in the 0.9 m separation case. At this point, the flame spread rate decreases abruptly. For the 1.8 m separation case, the flame spread rate is faster than for either 0.3 m or 0.9 m separation cases. It is decreasing as it reaches the end of the mulch pan at 1.8 m from the wall. The two experiments at 0 m separation from the wall show widely disparate flame spread rates, with one (#2) showing the same rate at the 1.8 m case until the flame front stalls at 0.4 m from the wall and the other (#8) showing the same rate as the final rate of 0.3 m and 0.9 m separation cases. The reasons for this behavior are not yet understood and will be studied further.

Right (R) and left (L) videos have been analyzed for 0.3 m, 0.9 m, and 1.8 m cases. The maximum difference between measured flame front locations at a given time is roughly 10 cm, which is in line with uncertainty estimates.

Figure 9. Flame front location with time as a function of separation distance for 10 m/s wind speed



Flame front locations for experiments at various separation distances at a wind speed of 14 m/s are plotted in Figure 10. Again, the behavior for 0.3 m and 0.9 m separation distances is similar. Here, the flame spread rate decreases more gradually from its maximum value after the start-up period, until the flame front slows significantly at a distance between 1.3 m and 1.7 m from the wall. The flame spread rate for the experiment at 1.8 m separation is comparable to the 0.3 m and 0.9 m separation cases at the same distance from the wall. Just as in the 10 m/s wind cases in Figure 9, the 0 m separation case behaves differently, showing a much slower flame spread rate throughout.

Figure 10. Flame front location with time as a function of separation distance for 14 m/s wind speed

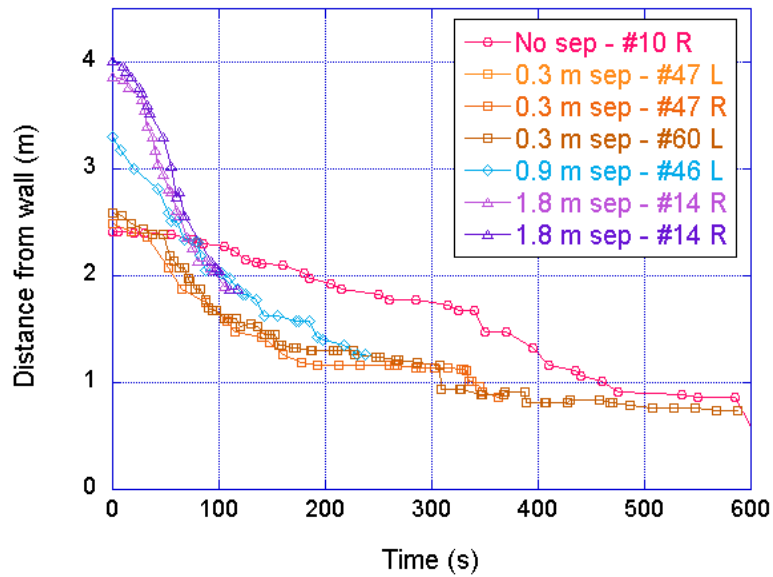


Figure 11 plots the flame front location with time for experiments at the same separation distance of 0.9 m and at three different wind speed settings. The flame spread rate after the start-up period (when the location of the flame front is about 2.8 m from the wall) is a function of wind speed, with slower flame spread rate corresponding to slower wind speed. In all cases, the flame spread rate changes abruptly at a distance of about 1.6 m from the wall.

Figure 11. Flame front location with time as a function of wind speed for 0.9 m separation distance

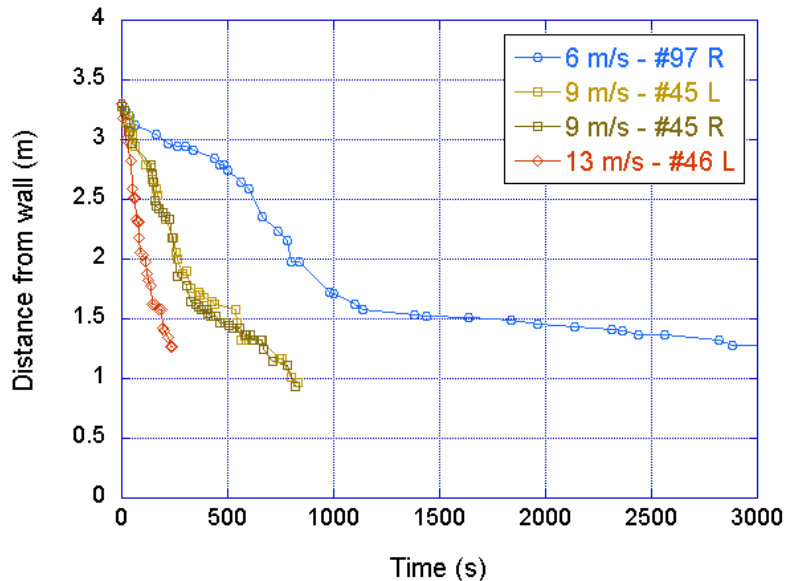
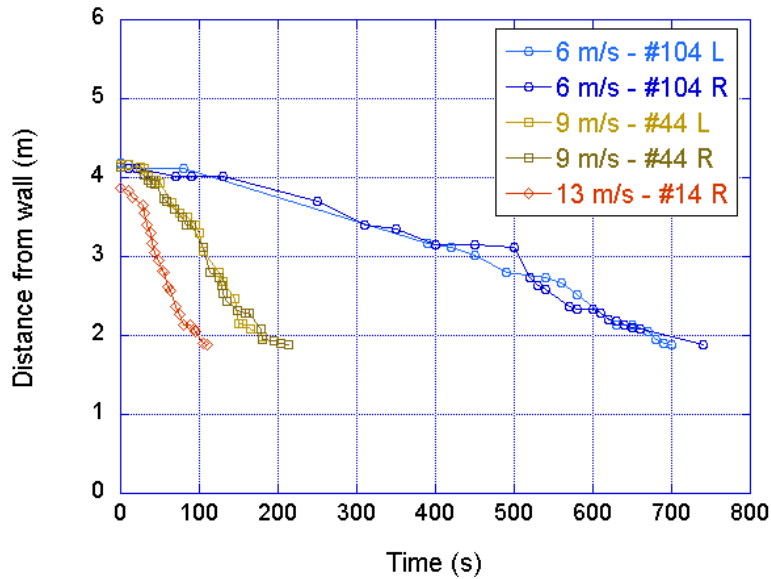


Figure 12 shows the flame front location with time for experiments at three different wind speed settings, all at a separation distance of 1.8 m. The flame spread rate after the start-up period is a function of wind speed, with slower flame spread rate corresponding to slower wind speed. Although the flame spread rate is slowing as the flame front reaches the end of the mulch, no abrupt decrease is observed.

Figure 12. Flame front location with time as a function of wind speed for 1.8 m separation distance



## COMPUTATIONAL ANALYSIS

The observation during this set of field experiments that the flame front consistently slowed as it approached the structure suggested that the flow field could be playing an important role. To obtain insights into the fire behavior, the experimental setup was modelled using the NIST Fire Dynamics Simulator (FDS),<sup>9</sup> a computational fluid dynamics (CFD) software program typically used for calculating fire-driven fluid flow in enclosures. As an initial exploration into the mulch bed experiments, FDS was used for calculating fluid flow only (no fire) in an exterior computational space with open boundaries. Subgrid mixing due to turbulence was represented by a Smagorinsky large eddy simulation (LES) model. Recent validation work<sup>10</sup> has showed that FDS is capable of good results when compared with experiments for similar problems, including building ventilation, wind impinging on the exterior of a structure, and transport of pollutants in an urban environment.

### Flow field results

In the model of the mulch test, illustrated in Figure 13, the fan and shed structure were represented as obstacles, shown in brown. Since the intent of the model was to provide insight rather than a quantitative comparison, the propeller-driven flow field and the geometries of the structure and the fan/flow straightener system were not represented in detail. The fan was simulated by a square block 1.8 m on a side and 0.5 m thick with a steady velocity boundary condition directed toward the structure at an angle of 7° to the horizontal. The distance of the fan from the structure was 10.7 m in agreement with the experimental setup. Boundary conditions at the exterior of the domain were open. Resolution in x, y, and z directions was 0.1 m.

Instantaneous velocity vectors in Fig. 13 illustrate some of the features of the wind flow, which is highly turbulent. Figures 13a and b show instantaneous velocity vectors along the center plane of the experimental geometry (side view) and in a plane 0.1 m above the ground (top view), respectively. The vectors are

colored by wind speed, with red corresponding to the maximum value of 9 m/s. The velocity flow field shows that a vortex forms near the ground in front of the structure and wraps around the sides, consistent with the horseshoe vortex observed for a surface-mounted cube in a flow field found in the literature.<sup>6</sup> The behavior of the wind near the ground is of particular interest for the mulch experiments. The side view in Figure 13a shows the vortex near the ground in front of the structure. In the top view in Figure 13b, the wind velocity just above the ground is high and directed toward the structure at distances between one and two structure heights (about 2 m to 7 m) from the structure. Within one structure height distance (about 2 m) from the structure, the wind velocity is lower and directed toward the fan.

The flow field strongly influences the behavior of firebrands generated in the mulch bed. Firebrands near the ground experience the opposing flow from the vortex, which acts to keep them away from the structure and directs them into the high velocity flow around the left or right side of the structure shown in Fig. 13b. Firebrands that are lofted to an intermediate height of 0.1 m to 1 m may be caught in the vortex flow and deposited close to the wall of the structure, where they can ignite combustible wall material or mulch adjacent to the wall. Firebrands that approach the structure at a height greater than a meter may enter an updraft that transports them over the top of the structure; open vents could allow these firebrands to enter the structure.

Figure 13. FDS model results showing instantaneous velocity vectors. Side view (a) shows velocities along the center plane, and top view (b) shows velocities in a plane 0.1 m above the ground.

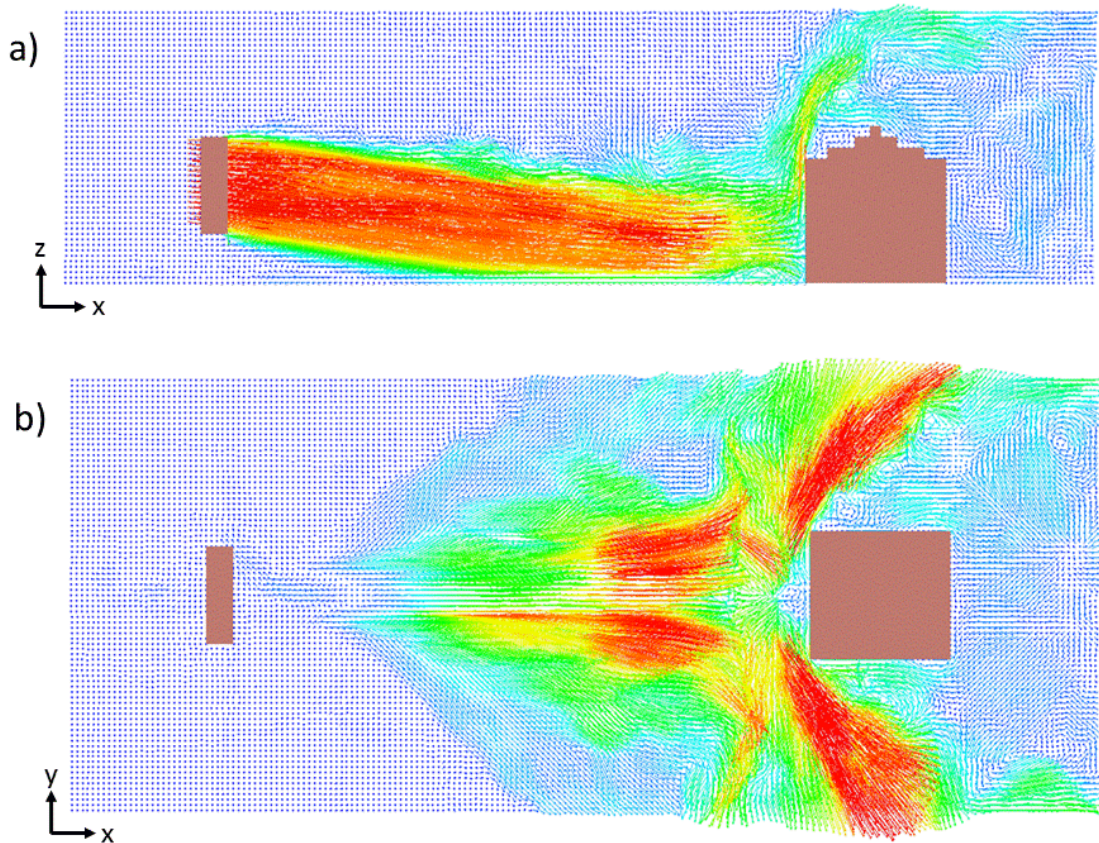


Figure 14 shows the x component of velocity  $v_x$ , in the direction toward or away from the structure, averaged over time. The size of the vortex is approximately 0.7 times the dimensions of the structure, roughly consistent with the literature on flow around surface-mounted cubes at high Re.<sup>7,8</sup> Between the fan

and the structure, the wind is directed toward the structure (positive values of  $v_x$ ) except for a region close to the ground just in front of the structure, where  $v_x$  is strongly negative (blue). Depending on how far away from the structure the mulch bed is ignited, the flames spreading toward the structure may initially experience concurrent flow, with wind velocity in the same direction as the flame spread. As the flame front enters the vortex region, however, the flame spread changes to opposed flow mode and slows considerably. If a firebrand ignites the mulch within the vortex region, as in Figure 5, the flame spread from the point of ignition back to the main flame front is concurrent with the vortex flow field, and is thus rapid.

Simulations at imposed wind speeds from 6 m/s to 14 m/s indicated that the vortex size is relatively independent of wind speed in this range. Vortex intensity and concurrent and opposed flow velocities are strongly affected by wind speed.

Figure 14. FDS model results showing time-averaged values of velocity  $v_x$  in the x direction. Side view (a) shows  $v_x$  along the center plane, and top view (b) shows  $v_x$  in a plane 0.1 m above the ground

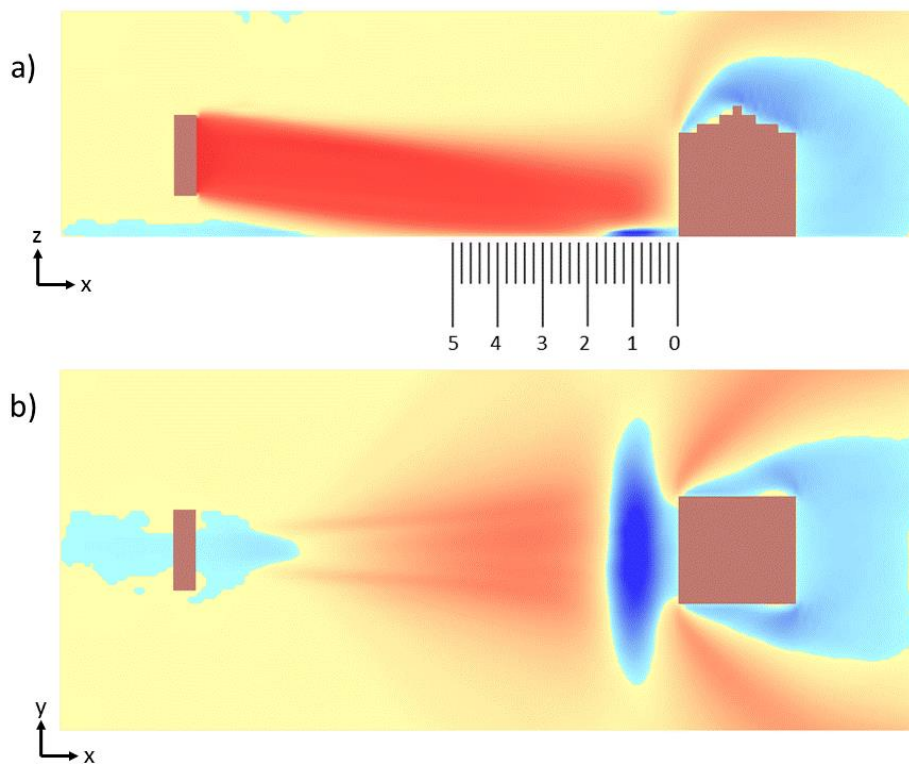


Figure 14a includes a scale marked from 0 m to 5 m away from the structure. This figure can be compared with Figures 8 through 12 showing flame front location with time to understand the changes in flame spread rate. For the mulch pan separated from the structure by 1.8 m, the flame spread takes place completely outside of the vortex. However, the concurrent velocity slows as the flame approaches the end of the mulch pan, which could explain the gradual decrease in flame spread rate. The flame fronts in mulch pans separated from the structure by 0.3 m and 0.9 m encounter the vortex as they approach the building, causing the flame spread to go from concurrent to opposed flow mode. This accounts for the abrupt change in flame spread rate at around 1.7 m from the structure. The flame front in a mulch pan that is adjacent to the structure with no spacing is primarily within the vortex. The lack of a transition in flame spread rate for a burning region ignited just outside of the vortex requires further study, as does a zero separation case that shows rapid flame spread.

## CONCLUSIONS

Field experiments have been carried out on flame spread in mulch pans at a variety of separation distances from a small building and at a variety of imposed wind speeds. The flame spread rates for mulch pans separated at 0.3 m and 0.9 m from the structure undergo an abrupt decrease between 1.3 m and 1.7 m from the structure. Simulations demonstrate that this change is due to the presence of a vortex near the ground in front of the structure, which causes the flame front to transition from concurrent to opposed flow modes. Flame spread rates for mulch pans at 1.8 m separation from the structure begin to slow near the end of the mulch pan but do not enter the vortex and do not change abruptly. Flame spread rates at a distance greater than the height of the structure are dependent on wind speed.

This work demonstrates how field experiments and modelling can lend insight into the physics underlying a recognized WUI fire hazard.

## REFERENCES

- <sup>1</sup> Fernandez-Pello, A.C. and Hirano, T. (1983). Controlling mechanisms of flame spread. *Combustion Science and Technology* 32, pp. 1-31
- <sup>2</sup> Pagni, P.J. and Peterson, T.G. (1973). Flame spread through porous fuels. In *Proceedings of the Fourteenth Symposium (International) on Combustion, 20-25 August 1972, University Park, PA*, pp. 1099-1107. (The Combustion Institute : Pittsburgh, PA).
- <sup>3</sup> Nelson Jr., R.M. (2015). Re-analysis of wind and slope effects on flame characteristics of Mediterranean shrub fires. *International Journal of Wildland Fire* 24, pp. 1001-1007. doi :10.1071/WF14155.
- <sup>4</sup> Delichatsios, M.A. (1996). Creeping flame spread : Energy balance and application to practical materials. In *Proceedings of the Twenty-Sixth Symposium (International) on Combustion, 28 July-2 August 1996, Naples, Italy*, pp. 1495-1503. (The Combustion Institute : Pittsburgh, PA).
- <sup>5</sup> Catchpole, W.R., Catchpole, E.A., Butler, B.W., Rothermel, R.C., Morris, G.A. and Latham, D.J. (1998). Rate of spread of free-burning fires in woody fuels in a wind tunnel, *Combustion Science and Technology* 131, pp. 1-37.
- <sup>6</sup> Hunt, J.C.R., Abell, C.J., Peterka, J.A. and Woo, H. (1978). Kinematical studies of the flows around free or surface-mounted obstacles; applying topology to flow visualization. *Journal of Fluid Mechanics* 86(1), pp. 179-200.
- <sup>7</sup> Martinuzzi, R. and Tropea, C. (1993). The flow around surface-mounted, prismatic obstacles placed in a fully developed channel flow. *Journal of Fluids Engineering* 115, pp. 85-92.
- <sup>8</sup> Sedighi, K. and Farhadi, M. (2006). Three-dimensional study of vortical structure around a cubic bluff body in a channel. *Facta Universitatis : Mechanical Engineering* 4(1), pp. 1-16.
- <sup>9</sup> McGrattan, K., McDermott, R., Weinschenk, C., Overholt, K., Hostikka, S. and Floyd, J. (2013). *Fire Dynamics Simulator User's Guide*. NIST Special Publication 1019, 6<sup>th</sup> ed. National Institute of Standards and Technology, Gaithersburg, MD.
- <sup>10</sup> McGrattan, K., Hostikka, S., McDermott, R., Floyd, J., Weinschenk, C., and Overholt, K. (2014). *Fire Dynamics Technical Reference Guide, Volume 3: Validation*. NIST Special Publication 1018, 6<sup>th</sup> ed. National Institute of Standards and Technology, Gaithersburg, MD.